Influence of radiative coupling on coherent Rabi intersubband oscillations in multiple quantum wells

Inès Waldmueller and Weng W. Chow
Sandia National Laboratories, Albuquerque, New Mexico 87185-0601, USA

Andreas Knorr
Institut für Theoretische Physik, Technische Universität Berlin, 10623 Berlin, Germany
(Received 27 September 2005; revised manuscript received 6 December 2005; published 27 January 2006)

The dependence of multiple quantum well intersubband Rabi oscillations on the radiative coupling between different quantum wells is investigated. We show that in a highly doped multiple quantum well sample, radiative coupling has a large impact on coherent density oscillations, even stronger than the impact of many-body effects. Specifically, radiative coupling can dominate nonlinear optical response, such as Rabi oscillations of subband populations, yielding distinctively different excitation behaviors in the different wells of a multiple quantum well sample. The magnitude of radiative coupling may be controlled by varying the angle of incidence of the external electric field.

DOI: 10.1103/PhysRevB.73.035433 PACS number(s): 73.21.Fg, 78.67.De

I. INTRODUCTION

Rabi oscillations is a much studied phenomena in ultrafast nonlinear optics: a driving electric field $E(t)$ couples two energy levels with optical dipole moment d_{12} and induces oscillations of the populations at the Rabi frequency $\Omega(t) = E(t)d_{12}/\hbar$.[1] Rabi oscillations are important for a broad range of technical applications such as quantum information processing. There is already considerable interest in Rabi oscillations involving *interband* dynamics of low-dimensional semiconductors such as quantum dots[2–5] and quantum wells.[6–8] Recently, the interest extends to *intersubband* systems, where Rabi oscillations between conduction subbands of a quantum well were observed experimentally[9] and addressed theoretically.[10,11] In this paper, we further the investigation of intersubband Rabi oscillations by examining coherent density oscillations in a highly doped multiple quantum well system. The reason for this study lies in recent experimental results which show substantial impact of radiative coupling on the nonlinear response of intersubband transitions in a multiple quantum well system. Shih *et al.*[12] used phase and amplitude resolved propagation studies on multiple quantum well samples with different carrier densities to demonstrate the dependence of the relationship between excitation amplitude and transmission on the strength of radiative coupling. Using a many-particle theory including light propagation effects, we were able to fully account for the experimental results. In this paper, we apply this theory to show that radiative coupling dominates over many-body effects when the system is excited by the electric pump field at a large angle of incidence.

At first sight, intersubband systems appear to have much in common with atomic two-level systems, because subbands with almost equal curvature (in-plane energy dispersion) give rise to a transition energy that is independent of the in-plane wave vector **k** [cf. Fig. 1(a)]. However, this simplified picture is valid only in a single-particle picture, i.e., by neglecting many-particle interactions. Early studies show that many-body effects reduce similarity to two-level systems drastically by introducing (i) carrier-carrier Hartree-Fock contributions,[13–15] yielding time-dependent renormalizations of subband dispersion and Rabi frequency, and (ii) dephasing due to carrier-carrier and carrier-phonon scattering.[15,16] Furthermore, nonparabolicity of the conduction band can have significant impact on the curvature of the subbands. The impact is strongest for small quantum wells,[17] resulting in different subband dispersions [cf. Fig. 1(b)] and thus a range of transition frequencies. All the above factors can influence the ability to produce Rabi oscillations and therefore the coherent nonlinear control of populations in quantum wells.[10,11]

This paper expands previous investigations by incorporating radiative coupling due to transversal fields (light propagation) between quantum wells in a highly doped multiple quantum well system. We find that radiative coupling can have an even stronger impact on Rabi oscillations of subband populations than dispersion and the above many-body effects associated with longitudinal Coulomb fields. Comparison of density oscillations are made for single and multiple quantum well samples. The multiple quantum well (MQW)

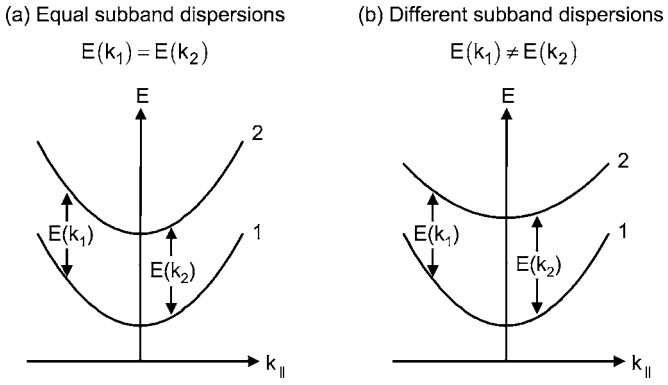

FIG. 1. (a) Intersubband transitions between subbands with equal subband dispersions and (b) different subband dispersions.

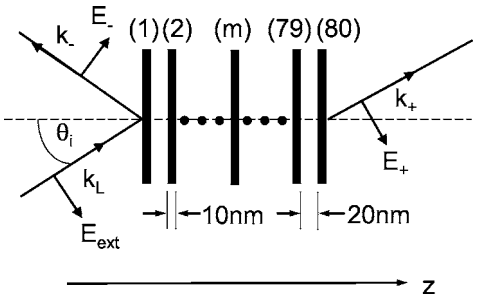

FIG. 2. Multiple quantum well system consisting of N electronically uncoupled wells excited by a p-polarized external electric field E^{ext} at angle of incidence θ_i. E_+ and E_- denote the right and left propagating *total* outgoing field, consisting of contributions from the external applied field and the fields generated by the polarization in the quantum wells.

sample of interest (cf. Fig. 2) contains 80 electronically uncoupled AlGaAs/GaAs quantum wells with a well width of $L=10$ nm. The wells are modulation doped with a carrier density of $n_e=10^{12}\ \text{cm}^{-2}$ and separated by $Al_{0.35}Ga_{0.65}As$ barriers with a thickness of 20 nm. The system is excited by an external p-polarized Gaussian pulse with three-dimensional (3D) wave vector

$$\mathbf{k}_L=(\mathbf{k}_\parallel^L,k_z^L)=\omega_i\sqrt{\epsilon_\infty\mu_0}(\sin(\theta_i),0,\cos(\theta_i)) \tag{1}$$

and laser frequency ω_L. ϵ_∞ denotes the optical permittivity, μ_0 the permeability of free space. To investigate the impact of radiative coupling on the density oscillations, we excite at different angles of incidence θ_i. We will show that for $\theta_i=23^\circ$ the wells are almost completely uncoupled, whereas for $\theta_i=63^\circ$ appreciable light propagation effects are observed. As will be clear later, the two angles of 23° and 63°, respectively, lead to weak and strong internal electric field contributions.

II. THEORY

Following semiclassical laser theory, we use a combination of density matrix approach for the material response (cf., for example, Refs. 15, 16, and 18) and Green's function approach for the propagating electric field in the structure.[20]

A. Matter

Taking into account optical transitions between the two lowest conduction subbands, the polarization density in quantum well m in a multiple quantum well system composed of N electronically uncoupled quantum wells is given by

$$\mathbf{P}^{(m)}(\mathbf{r},t)=\sum_{\mathbf{q}_\parallel}\tilde{\mathbf{P}}^{(m)}(\mathbf{q}_\parallel,z,t)e^{i\mathbf{q}_\parallel\cdot\mathbf{r}_\parallel} \tag{2}$$

with

$$\tilde{\mathbf{P}}^{(m)}(\mathbf{q}_\parallel,z,t)=\frac{1}{A}\sum_{\mathbf{k}_\parallel}p^{(m)}_{\mathbf{k}_\parallel-\mathbf{q}_\parallel,\mathbf{k}_\parallel}(t)\mathbf{d}^{(m)}_{12}(z)+\text{c. c.} \tag{3}$$

Here $p^{(m)}_{\mathbf{k}_\parallel-\mathbf{q}_\parallel,\mathbf{k}_\parallel}(t)=\langle a^\dagger_{1,\mathbf{k}_\parallel-\mathbf{q}_\parallel}a_{2,\mathbf{k}_\parallel}\rangle^{(m)}$ is the time dependent expectation value of creating an electron with two-dimensional (2D) vector $(\mathbf{k}_\parallel-\mathbf{q}_\parallel)$ in subband 1 and annihilating an electron with wave vector $\mathbf{k}_\parallel$ in subband 2 (intersubband coherence). The superscript (m) denotes the quantum well in which the transition occurs. If not stated otherwise, the spin index is absorbed in the in-plane wave vector. The spatial distribution of the dipole density is abbreviated by $\mathbf{d}^{(m)}_{12}(z)=d^{(m)}_{12}(z)\hat{\mathbf{e}}_\mathbf{z}=-ez\phi^{(m)}_1(z)\phi^{(m)}_2(z)\hat{\mathbf{e}}_\mathbf{z}$ with $\phi^{(m)}_a(z)$ being the ath level confinement wave function of the mth quantum well. The system Hamiltonian is given by

$$\begin{aligned}H=&\sum_{a,\mathbf{k}_\parallel}\epsilon_{a\mathbf{k}_\parallel}a^\dagger_{a\mathbf{k}_\parallel}a_{a\mathbf{k}_\parallel}\\&+\sum_{a,b}\sum_{\mathbf{k}_\parallel,\mathbf{q}_\parallel}\int dz\mathbf{d}_{ab}(z)\cdot\tilde{E}_T(\mathbf{q}_\parallel,z,t)a^\dagger_{a\mathbf{k}_\parallel+\mathbf{q}_\parallel}a_{b\mathbf{k}_\parallel}\\&+\sum_{a,b,c,d}\sum_{\mathbf{k}_\parallel,\mathbf{k}'_\parallel,\mathbf{q}_\parallel}(\hat{V}^{acbd}_{\mathbf{q}_\parallel}\langle a^\dagger_{c\mathbf{k}'_\parallel-\mathbf{q}_\parallel}a_{d\mathbf{k}'_\parallel}\rangle a^\dagger_{a\mathbf{k}_\parallel+\mathbf{q}_\parallel}a_{b\mathbf{k}_\parallel}\\&-\hat{V}^{cabd}_{\mathbf{q}_\parallel}\langle a^\dagger_{c\mathbf{k}_\parallel+\mathbf{q}_\parallel}a_{d\mathbf{k}'_\parallel}\rangle a^\dagger_{a\mathbf{k}'_\parallel-\mathbf{q}_\parallel}a_{b\mathbf{k}_\parallel})\\&+\sum_{a,b,\mathbf{k}_\parallel}\sum_{\mathbf{q}}[\hat{g}^{ab}_{\mathbf{q}}a^\dagger_{a\mathbf{k}_\parallel}b_{\mathbf{q}}a_{b\mathbf{k}_\parallel-\mathbf{q}_\parallel}+\text{h. a.}],\end{aligned} \tag{4}$$

where $\epsilon_{a\mathbf{k}_\parallel}$ denotes the energy of an electron in subband a with 2D in-plane wave vector $\mathbf{k}_\parallel$, $a^\dagger_{c\mathbf{k}_\parallel}(a_{c\mathbf{k}_\parallel})$ is the creation (annihilation) operator for an electron in subband c with wave vector $\mathbf{k}_\parallel$ and $b^\dagger_\mathbf{q}(b_\mathbf{q})$ is the creation (annihilation) operator for a phonon with the 3D wave vector $\mathbf{q}$. The Coulomb and Fröhlich coupling matrix elements are given in Eq. (B2) in Ref. 15 and we have reduced the Coulomb Hamiltonian to the corresponding screened Hartree-Fock form. For the carrier-field interaction $\tilde{E}_T(\mathbf{q}_\parallel,z,t)$ denotes the Fourier transform of the transverse part of the electric field $E_T(\mathbf{r},t)$ with respect to in-plane space coordinates $\mathbf{r}_\parallel$,

$$\tilde{E}_T(\mathbf{q}_\parallel,z,t)=\frac{1}{2\pi}\int d^2r_\parallel e^{-i\mathbf{q}_\parallel\cdot\mathbf{r}_\parallel}E_T(\mathbf{r},t), \tag{5}$$

where $E_T(\mathbf{r},t)$ is the total (external and internal) electric field inside the sample. Note, that only the transverse part of the field enters the microscopic equations as the longitudinal part is already included in the Coulomb interaction (Coulomb gauge). In the Hamiltonian, we include electrons, longitudinal-optical (LO) phonons and carrier-field interaction. Furthermore, we investigate the dependence of radiative effects on other dephasing contributions by including electron-LO-phonon interaction, where the phonons are treated as a thermal reservoir at temperature T. Note that we consider only the Markovian contributions (non-Markovian effects in single quantum wells are given in Ref. 22). Due to their enormous CPU time requirement, electron-electron interaction is included in first order (Hartree-Fock effects) only. A simultaneous treatment of carrier-carrier (Hartree-Fock and scattering), carrier-phonon interaction and radiative damping in the *linear regime* is presented in Refs. 14, 15, and 19, and without radiative interaction in Ref. 16. In this paper, our focus is on the radiative coupling.

Using the Robertson equation[21] and the system Hamiltonian, we derive an equation of motion for the intersubband

coherence in the mth quantum well $p^{(m)}_{\mathbf{k}_\parallel-\mathbf{Q}_\parallel,\mathbf{q}_\parallel}(t)$.[15]

To include radiative coupling, i.e., the coupling between the wells via the transverse electric field, in the theory, we must consider the actual space-dependent field (determined by Maxwell's equations) in the equations of motion which yields an in-plane space-dependent macroscopic polarization. However, we can simplify the space dependence to a large extent by concentrating on the dominant in-plane contributions driven directly by the external field. In the parameter range considered here [cf. Eq. (A4) with Eq. (1), $\hbar\omega_L \approx 90-110$ meV, $\tau=100$ fs] this yields a macroscopic polarization composed of intersubband coherences which are diagonal in the in-plane wave vector (the derivation is given in Appendix A):

$$\mathbf{P}(\mathbf{r},t) = \frac{1}{\sqrt{2\pi}}\int_{-\infty}^{\infty} d\omega \sum_{\mathbf{q}_\parallel} \hat{\mathbf{P}}(\mathbf{q}_\parallel,z,\omega) e^{i(\mathbf{q}_\parallel\cdot\mathbf{r}_\parallel-\omega t)} \tag{6}$$

with

$$\hat{\mathbf{P}}(\mathbf{q}_\parallel,z,\omega) \approx \hat{\mathbf{P}}(z,\omega)\delta_{\mathbf{q}_\parallel\omega_L,\omega\mathbf{k}_\parallel^L}, \tag{7}$$

$$\begin{aligned}\hat{\mathbf{P}}(z,\omega) &= \frac{1}{A}\sum_{\mathbf{k}_\parallel,m}[p^{(m)}_{\mathbf{k}_\parallel-\frac{\omega}{\omega_L}\mathbf{k}_\parallel^L,\mathbf{k}_\parallel}(\omega) + \text{c . c . }]\mathbf{d}_{12}(z)\\ &\approx \frac{1}{A}\sum_{\mathbf{k}_\parallel,m}[p^{(m)}_{\mathbf{k}_\parallel}(\omega) + \text{c . c . }]\mathbf{d}_{12}(z).\end{aligned} \tag{8}$$

Here, the abbreviation $p^{(m)}_{\mathbf{k}_\parallel} \equiv p^{(m)}_{\mathbf{k}_\parallel,\mathbf{k}_\parallel} = \langle a^\dagger_{1,\mathbf{k}_\parallel} a_{2,\mathbf{k}_\parallel}\rangle^{(m)}$ has been introduced.

The equation of motion for the intersubband coherence is coupled to the equations of motion for the carrier distribution functions $n^m_{i,\mathbf{k}_\parallel}(t) = \langle a^\dagger_{i,\mathbf{k}_\parallel} a_{i,\mathbf{k}_\parallel}\rangle^{(m)}(t)$ in the two subbands ($i=1,2$), where we distinguish between free-carrier ($|_0$), carrier-field ($|_{\text{cf}}$), Hartree-Fock contributions ($|_{\text{HF}}$) and scattering contributions due to carrier-phonon interaction ($|_{\text{scatt}}$),

$$\begin{aligned}\frac{d}{dt}p^{(m)}_{\mathbf{k}_\parallel}(t) &= \left.\frac{d}{dt}p^{(m)}_{\mathbf{k}_\parallel}(t)\right|_0 + \left.\frac{d}{dt}p^{(m)}_{\mathbf{k}_\parallel}(t)\right|_{\text{cf}} + \left.\frac{d}{dt}p^{(m)}_{\mathbf{k}_\parallel}(t)\right|_{\text{HF}}\\ &\quad + \left.\frac{d}{dt}p^{(m)}_{\mathbf{k}_\parallel}(t)\right|_{\text{scatt}},\end{aligned}$$

$$\frac{d}{dt}n^{(m)}_{2,\mathbf{k}_\parallel}(t) = \left.\frac{d}{dt}n^{(m)}_{i,\mathbf{k}_\parallel}(t)\right|_{\text{cf}} + \left.\frac{d}{dt}n^{(m)}_{i,\mathbf{k}_\parallel}(t)\right|_{\text{HF}} + \left.\frac{d}{dt}n^{(m)}_{i,\mathbf{k}_\parallel}(t)\right|_{\text{scatt}}. \tag{9}$$

$|_0$ describes the free motion of the electrons, $|_{\text{cf}}$ the interaction with the z component of the transverse electric field (Rabi frequency) in dipole approximation. $|_{\text{HF}}$ yields renormalizations of $|_0$ and $|_{\text{cf}}$ due to carrier-carrier interaction (first order contributions, Hartree-Fock approximation) and $|_{\text{scatt}}$ carrier-phonon scattering and thus introduces optical dephasing on a microscopic basis. A derivation of this part of the theory can be found in Refs. 15 and 19. We here give only the carrier-field interaction,

$$\left.\frac{d}{dt}p^{(m)}_{\mathbf{k}_\parallel}\right|_{\text{cf}} = \frac{\mathrm{i}}{\hbar}\sum_{\mathbf{q}_\parallel}\int dz \tilde{E}_{T,z}(\mathbf{q}_\parallel,z,t) d^{(m)}_{12}(z)[\langle a^\dagger_{1,\mathbf{k}_\parallel+\mathbf{q}_\parallel} a_{1,\mathbf{k}_\parallel}\rangle^{(m)} - \langle a^\dagger_{2,\mathbf{k}_\parallel} a^\dagger_{2,\mathbf{k}_\parallel-\mathbf{q}_\parallel}\rangle^{(m)}], \tag{10a}$$

$$\left.\frac{d}{dt}n^{(m)}_{1,\mathbf{k}_\parallel}\right|_{\text{cf}} = -\frac{2}{\hbar}\sum_{\mathbf{q}_\parallel}\int dz \tilde{E}_{T,z}(\mathbf{k}^L_\parallel,z,t) d^{(m)}_{12}(z)[\langle a^\dagger_{1,\mathbf{k}_\parallel+\mathbf{q}_\parallel} a_{2,\mathbf{k}_\parallel}\rangle^{(m)} - \langle a^\dagger_{1,\mathbf{k}_\parallel} a^\dagger_{2,\mathbf{k}_\parallel-\mathbf{q}_\parallel}\rangle^{(m)}], \tag{10b}$$

$$\left.\frac{d}{dt}n^{(m)}_{2,\mathbf{k}_\parallel}\right|_{\text{cf}} = \frac{2}{\hbar}\sum_{\mathbf{q}_\parallel}\int dz \tilde{E}_{T,z}(\mathbf{k}^L_\parallel,z,t) d^{(m)}_{12}(z)[\langle a^\dagger_{1,\mathbf{k}_\parallel+\mathbf{q}_\parallel} a_{2,\mathbf{k}_\parallel}\rangle^{(m)} - \langle a^\dagger_{1,\mathbf{k}_\parallel} a^\dagger_{2,\mathbf{k}_\parallel-\mathbf{q}_\parallel}\rangle^{(m)}]. \tag{10c}$$

$\tilde{E}_{T,z}(\mathbf{q}_\parallel,z,t)$ is the z component of the transverse electric field [Fourier transformed with respect to in-plane space coordinates, cf. Eq. (5)] which must be determined self-consistently by taking into account the external and internal emitted fields. The other contributions of Eq. (9) are given in Appendix B.

B. Self-consistent optical field

To calculate the internally emitted electric fields, the solution of Maxwell's equations must be combined with the equation for the polarization density: in Eq. (10) the *actual local* field consisting of externally incident field and remitted fields generated by the material polarization in the MQW sample must be considered. Based on the solutions of Maxwell's equations in Fourier domain (Greens function formalism[15,23,20]), we obtain the z component of the total electric field (transversal and longitudinal components) generated by the polarization density of the quantum wells by Fourier superposition,

$$E^{\text{pol}}_z(\mathbf{r},t) = \frac{1}{2\pi}\int d^2q_\parallel e^{i\mathbf{q}_\parallel\cdot\mathbf{r}_\parallel}\tilde{E}^{\text{pol}}_z(\mathbf{q}_\parallel,z,t), \tag{11}$$

$$\begin{aligned}\tilde{E}^{\text{pol}}_z(\mathbf{q}_\parallel,z,t) &= \frac{1}{\sqrt{2\pi}}\int_{-\infty}^{\infty} d\omega e^{-i\omega t}\sum_{m=1}^{N}\int dz' \hat{P}^{(m)}_z(\mathbf{q}_\parallel,z',\omega)\\ &\quad\times\left(\frac{i\mu_0\omega^2}{2q_\perp}\frac{q_\parallel^2}{q^2}e^{iq_\perp|z-z'|}[\Theta(z-z')\right.\\ &\quad\left.+\Theta(z'-z)] - \frac{1}{\epsilon_\infty}\delta(z-z')\right).\end{aligned} \tag{12}$$

Using the approximation given in Eq. (8) and

$$q_\perp = \sqrt{\omega^2\epsilon_\infty\mu_0 - q_\parallel^2},$$

we obtain the reemitted electric field as

$$\tilde{E}_z^{\mathrm{pol}}(\mathbf{q}_\parallel,z,t) \approx -\frac{1}{\sqrt{2\pi}}\int_{-\infty}^{\infty} d\omega \sum_{m=1}^{N} \int dz' \hat{P}_z^{(m)}(z',\omega) \times \left(\frac{\mu_0 \omega_L}{2k_z^L} \sin^2\theta_L \frac{d}{dt} e^{-i\omega[t-(k_z^L/\omega_L)|z-z'|]} [\Theta(z-z') + \Theta(z'-z)] + \frac{1}{\epsilon_\infty}\delta(z-z')e^{-i\omega t} \right) \delta_{\mathbf{q}_\parallel, \frac{\omega}{\omega_L}\mathbf{k}_\parallel^L}. \quad (13)$$

Next, we insert the transverse part of the total electric field in Eq. (10), i.e., the *transverse part of Eq. (13)* together with the external applied field $\tilde{E}_z^{\mathrm{ext}}(\mathbf{q}_\parallel,z,\omega)$ [cf. Eq. (A5)] and notice that for the parameter range considered, $(\omega/\omega_L)\mathbf{k}_\parallel^L \ll \mathbf{k}_\parallel$. Thus we can approximate

$$\langle a^\dagger_{i,\mathbf{k}_\parallel} a^\dagger_{j,\mathbf{k}_\parallel \pm (\omega/\omega_L)\mathbf{k}_\parallel^L} \rangle^{(m)} \approx \langle a^\dagger_{i,\mathbf{k}_\parallel} a^\dagger_{j,\mathbf{k}_\parallel} \rangle^{(m)}$$

yielding

$$\left.\frac{d}{dt} p^{(m)}_{\mathbf{k}_\parallel}\right|_{\mathrm{cf}} = \frac{\mathrm{i}}{\hbar}\int dz d_{12}^{(m)}(z)\mathcal{E}_{T,z}(z,t)[n^{(m)}_{1,\mathbf{k}_\parallel} - n^{(m)}_{2,\mathbf{k}_\parallel}], \quad (14)$$

$$\left.\frac{d}{dt} n^{(m)}_{i,\mathbf{k}_\parallel}\right|_{\mathrm{cf}} = \pm\frac{2}{\hbar}\int dz d_{12}^{(m)}(z)\mathcal{E}_{T,z}(z,t)\mathrm{Im}(p^{(m)}_{\mathbf{k}_\parallel}), \quad (15)$$

where $\mathcal{E}_{T,z}(z,t)$ is the transverse part of the total electric field composed of the external applied field [cf. Eqs. (A4) and (A5)] and the generated contributions

$$\mathcal{E}_z^{\mathrm{pol}}(z,t) = \sum_{m=1}^{N}\int dz' \left[-\frac{1}{\epsilon_\infty}\delta(z-z')P_z^{(m)}(z',t) - \frac{\mu_0\omega_L}{2k_z^L}\sin^2\theta_L \frac{d}{dt} P_z^{(m)}\left(z', t-\frac{k_z^L}{\omega_L}|z-z'|\right)\right]. \quad (16)$$

The influence of radiative coupling can be investigated by solving the microscopic equations (14) and (15) for every quantum well with the total radiation field.

III. NUMERICAL RESULTS

To determine the importance of radiative coupling in comparison to other effects, we investigate the temporal behavior of the relative population $(\Sigma_{\mathbf{k}} n_{2,\mathbf{k}}/n_e)$ in the upper subband in each well in a multiple quantum well system, with and without the dephasing, Hartree-Fock and nonparabolicity contributions. The system is composed of 80 electronically uncoupled quantum wells. Each 10 nm AlGaAs/GaAs quantum well is modulation doped with a carrier density of $n_e = 10^{12}$ cm^{-2} at a lattice temperature of $T = 50$ K (temperature of the thermal reservoir of phonons). The quantum wells are separated by $Al_{0.35}Ga_{0.65}As$ barriers with thickness of $D-L=20$ nm (Fig. 2). For the numerical simulations we use a square-well potential model with a finite height of $V_0 = 350$ meV and assume the system to be in thermal equilibrium before being excited by the external field. The external field is a Gaussian pulse [cf. Eq. (A4) and Fig. 2] with pulse width $\tau = 100$ fs. For the following application we characterize the strength of the electron-light interaction by the pulse area:

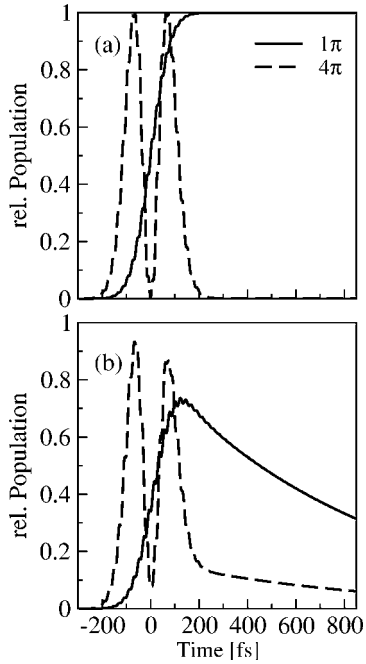

FIG. 3. Relative population in upper subband $(\Sigma_{\mathbf{k}} n_{2\mathbf{k}}/n_e)$ for a single quantum well for the two scenarios (a) and (b) (cf. text). Scenario (a) is comparable to a two-level system and thus perfect Rabi oscillations are possible. Scenario (b) takes into account many-particle contributions and nonparabolicity effects which both reduce the similarities to a two-level system. Only damped oscillations can be observed.

$$\Theta(z) := \frac{\mu_{12}}{\hbar}\int_{-\infty}^{\infty} dt |\mathcal{E}_z^{\mathrm{ext,s}}(z,t)|.$$

Here $\mathcal{E}_z^{\mathrm{ext,s}}(z,t)$ is the slowly varying envelope of $\mathcal{E}_z^{\mathrm{ext}}(z,t)$ and $\mu_{12} = \int_L dz d_{12}(z)$ is the dipole matrix element. We consider two different scenarios.

In scenario (*a*), we neglect nonparabolicity $(m_1 = m_2 = 0.0665 m_0)$, Hartree-Fock and scattering effects. The equations of motions are so that

$$\frac{d}{dt} p^{(m)}_{\mathbf{k}_\parallel}(t) = \left.\frac{d}{dt} p^{(m)}_{\mathbf{k}_\parallel}(t)\right|_{0,\mathrm{cf}}, \quad \frac{d}{dt} n^{(m)}_{i,\mathbf{k}_\parallel}(t) = \left.\frac{d}{dt} n^{(m)}_{i,\mathbf{k}_\parallel}(t)\right|_{\mathrm{cf}},$$

we have noninteracting single-particle excitations in a system with a transition energy independent of the in-plane wave vector $\mathbf{k}$.

In scenario (*b*) we consider nonparabolicity effects in effective mass approximation as presented in Ref. 17 $(m_1 = 0.071 m_0, m_2 = 0.088 m_0)$, and take into account contributions from Hartree-Fock and carrier-phonon scattering.

To characterize the response without radiative coupling of different wells, we focus first on the response of a single well (cf. Fig. 3). In scenario (a) the quantum well reacts like an undamped two level system, when excited resonantly $(\omega_L = \omega_G$ where ω_G is the gap energy at $\mathbf{k}=0$ between the subbands) by a Gaussian pulse with pulse area $\Theta = \pi$, all elec-

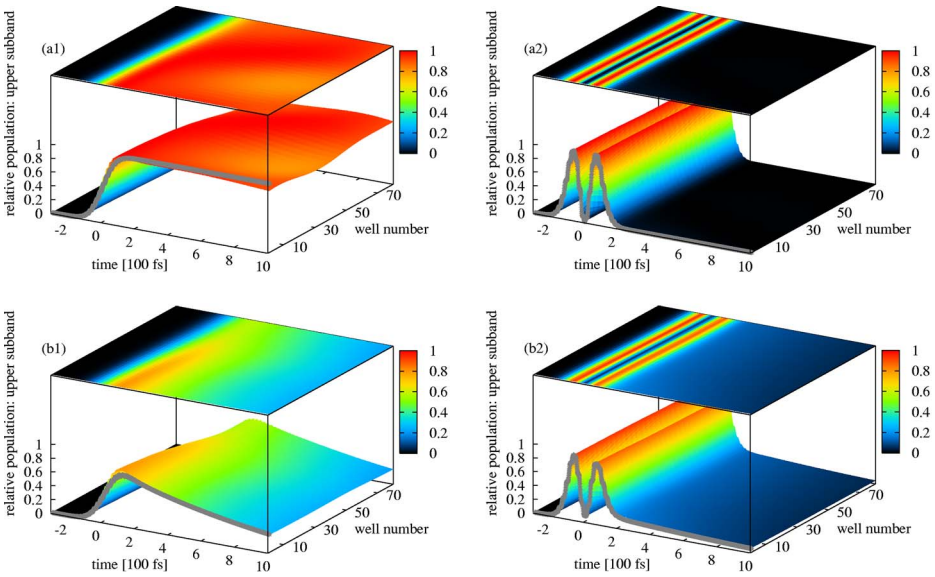

FIG. 4. (Color online) Relative population in the upper subband in each quantum well of a 80 quantum well sample excited at a small angle of incidence for models (a) and (b). Figures in the left column show the results of excitation by a pulse with pulse area $\Theta = 1\pi$, in the right column for $\Theta = 4\pi$. The thick, grey curve in the front shows the single quantum well result (cf. with Fig. 3).

trons are excited to the upper subband. In the case of $\Theta = 4\pi$, the electrons exhibit two complete Rabi periods. In scenario (b), the oscillations are suppressed by the inhomogeneous broadening due to the nonparabolicity, the Hartree-Fock effects and most importantly by carrier-phonon interaction. The Hartree-Fock effects introduce strong wave vector and time dependences of the transition energy and effective Rabi frequency. The exchange shift yields time and wave-vector-dependent effective transition energies of the electrons, making it impossible to excite resonantly at all times (even for systems with parabolic conduction band). The excitonic contribution yields an internal field due to interaction between carriers in different subbands which renormalizes the Rabi frequency. The renormalized Rabi frequency depends on the intersubband coherence, which in turn is driven by the Rabi frequency. Therewith, the renormalized Rabi frequency depends not only on time and wave vector, but also on laser frequency and pulse duration of the exciting field. Finally, the depolarization shift, also depends on laser frequency and pulse duration of the exciting field and introduces a second time-dependent renormalization of the Rabi frequency, which counteracts the impact of the excitonic contribution. By deliberately detuning the laser frequency from the gap frequency, the impact of these many-body effects on the density oscillations can be varied appreciably. Here, we choose the laser energy $\hbar\omega_L = \hbar\omega_G + 1$ meV to yield maximum oscillation amplitude. The new laser energy is roughly the intermediate between the initial gap energy and the peak position of the linear absorption spectrum.

Next, we consider the full system with all 80 quantum wells. To investigate the dependence of optical response on the strength of radiative coupling, we compare results for two different angles of incidence, $\theta_i = 23°$ and 63° (cf. Fig. 2). In order to have comparable situations, we choose the amplitude of the external field to yield the same $\mathcal{E}_z^{\text{ext}}(z,t)$ for both cases (if we excite at the small angle of incidence, the amplitude of the external field must be larger than for the excitation at a larger angle of incidence), cf. Eq. (A4). The field contribution of the *external field* in Eq. (14) and (15) is thus the same in both cases. However, as can be seen in Eq. (16), the expression for the generated field depends directly on the angle of incidence. Consequently, the *internal* field contributions are very different in the two cases. For decreasing angle of incidence, the internal field contributions decrease. Consequently, the Rabi oscillations in the different wells are similar. The quantum wells are only radiatively coupled by very small internal fields. In Fig. 4, we present the density oscillations in the upper subband for each quantum well of the sample. For direct comparison, the results for the single quantum well case (cf. Fig. 3) are plotted in the front. As can be seen, the single and multiple quantum well results are similar.

In contrast, Fig. 5 shows distinct differences between the single and MQW behavior for excitation at a larger angle of incidence. Due to strong internal field contributions, the local electrical field exhibits strong spatial dependence. For small pulse area (π pulse), reemitted fields dominate the oscillations at all times: a strong local electrical field excites all electrons to the upper subband in the first quantum wells. As the electric field weakens, the subsequent well populations are predominately in the lower subband. For large pulse area (4π pulse) the reemitted fields become visible only at the end of the external excitation. During the duration of the external excitation, the external field is stronger than the internal field yielding almost the same excitation in all wells. At the end of the external excitation, the impact of the reemitted fields becomes visible. Although the external field has almost completely decayed, reemitted field contributions are strong enough to excite electrons into the second subband. A third population peak appears between 200 and 400 fs. This third peak is absent for a single quantum well, as it is due only to internal field effects, i.e., fields reemitted by the other quantum wells.

The same results are obtained for scenario (b). The only difference between (a) and (b) is a slightly reduced overall excitation due to many-particle contributions and nonparabolicity effects. However, the impact of radiative coupling on the density oscillations is still dominant, as in scenario (a).

The results obtained for excitation at $\theta = 23°$ and 63° show the strong angle dependence of radiative coupling. This de-

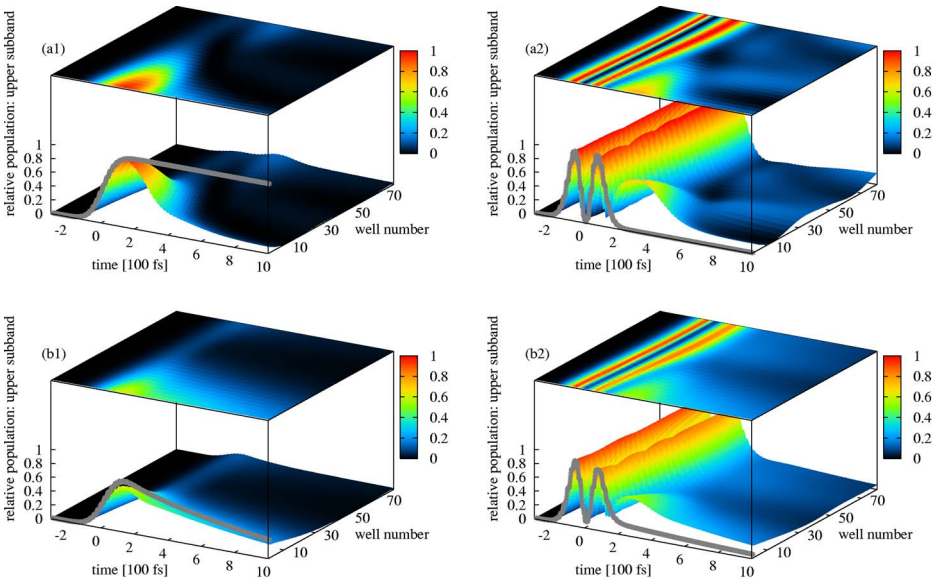

FIG. 5. (Color online) Relative population in the upper subband in each quantum well of a 80 quantum well sample excited at a large angle of incidence for models (a) and (b). As in Fig. 4, figures in the left column show the results of excitation by a pulse with pulse area $\Theta=\pi$, in the right column for $\Theta=4\pi$ and in all cases, the population excited in a sample containing only a single quantum well, is plotted additionally in the front (grey line, cf. with Fig. 3).

pendence may be understood by examining the limits of (a) normal incidence ($\theta_i=0°$) and (b) grazing incidence ($\theta_i=90°$). Approaching normal incidence, the z component of the field vanishes, thus, the light-matter interaction is very weak. Approaching grazing incidence, the z component of the field is very large, yielding strong light-matter interaction. However, in this case, the z component of the wave vector vanishes, so that the field does not propagate along the growth direction of the multiple quantum well system. Consequently, the wells are not coupled by the field. Between $\theta_i=0°$ and $\theta_i=90°$, the coupling to the field increases with $\sin\theta_i$ and the z component decreases with $\cos\theta_i$ yielding a strong angle dependence of the radiative coupling effects.

IV. CONCLUSION

In conclusion, we showed that radiative coupling between quantum wells of a multiple quantum well system can dominate nonlinear optical response, such as Rabi oscillations of subband populations. Especially for samples with high internal field contributions due to large carrier density and large angle of incidence, radiative coupling between wells yields distinctively different excitation behaviors in the different wells.

Generally, the impact of radiative coupling depends mostly on the relation of external and generated fields. If the external field is considerably larger than the generated field, local field effects are unimportant. The internal field amplitude depends on the carrier-density in the quantum wells and the excitation angle. Especially interesting is the case of highly doped multiple quantum well samples where the response of the MQW depends strongly on the angle of incidence.

For a small angle of incidence, where the internal field is small, the impact of radiative coupling is almost negligible (see, e.g., π and 4π pulse in Fig. 4). All the quantum wells are uniformly excited and there is almost no difference in the oscillations of a single and MQW sample. In contrast, excitation at large angle of incidence shows strong radiative coupling effects (cf. Fig. 5), with significant difference in the Rabi oscillations of a single and MQW sample.

ACKNOWLEDGMENTS

This work is funded by the Deutsche Forschungsgemeinschaft and the US Department of Energy under Contract No. DE-AC04-94AL8500. One of the authors (I.W.) acknowledges financial support by the "Berliner Programm zur Förderung von Frauen in Forschung und Lehre." One of the authors (W.C.) acknowledges support from the Senior Scientist Award of the Alexander von Humboldt Foundation. The authors thank M. Wörner, K. Reimann (Max-Born Institute, Berlin), and S. Butscher (TU Berlin) for stimulating discussions.

APPENDIX A

In this appendix, we show how the actual space dependence of the field can be simplified to a large extent by concentrating on the dominant in-plane contributions driven directly by the external field. This yields a macroscopic polarization composed of intersubband coherences which are diagonal in the in-plane wave vector [cf. Eqs. (6)–(8)]. The polarization density in quantum well m in a multiple quantum well system composed of N electronically uncoupled quantum wells is given by

$$\mathbf{P}^{(m)}(\mathbf{r},t)=\sum_{\mathbf{q}_\parallel}\tilde{\mathbf{P}}^{(m)}(\mathbf{q}_\parallel,z,t)e^{i\mathbf{q}_\parallel\cdot\mathbf{r}_\parallel} \tag{A1}$$

with

$$\tilde{\mathbf{P}}^{(m)}(\mathbf{q}_\parallel,z,t)=\frac{1}{A}\sum_{\mathbf{k}_\parallel}p^{(m)}_{\mathbf{k}_\parallel-\mathbf{q}_\parallel,\mathbf{k}_\parallel}(t)\mathbf{d}^{(m)}_{12}(z)+\text{c. c.} \tag{A2}$$

In order to simplify the in-plane space dependence of the polarization, we focus on the carrier-field contribution to the equation of motion for the intersubband coherence,

$$\frac{d}{dt}\langle a^{\dagger}_{1,\mathbf{k}_\parallel-\mathbf{k}'_\parallel}a_{2,\mathbf{k}_\parallel}\rangle = \frac{\mathrm{i}}{\hbar}\sum_{\mathbf{q}_\parallel}\int dz d_{12}(z)\tilde{E}_{z,T}(\mathbf{q}_\parallel,z,t) \times\left(\langle a^{\dagger}_{1,\mathbf{k}_\parallel-\mathbf{k}'_\parallel+\mathbf{q}_\parallel}a_{1,\mathbf{k}_\parallel}\rangle - \langle a^{\dagger}_{2,\mathbf{k}_\parallel-\mathbf{k}'_\parallel}a_{2,\mathbf{k}_\parallel-\mathbf{q}_\parallel}\rangle\right). \tag{A3}$$

Assuming initial homogenous electron distributions, i.e.,

$$\langle a^{\dagger}_{1,\mathbf{k}_\parallel-\mathbf{k}'_\parallel+\mathbf{q}_\parallel}a_{1,\mathbf{k}_\parallel}\rangle(t_0) = \langle a^{\dagger}_{1,\mathbf{k}_\parallel}a_{1,\mathbf{k}_\parallel}\rangle(t_0)\,\delta_{\mathbf{k}_\parallel-\mathbf{k}'_\parallel-\mathbf{q}_\parallel,\mathbf{k}_\parallel},$$

we find that only for intersubband coherences with $\mathbf{k}'_\parallel=\mathbf{q}_\parallel$ the dynamics is driven directly by the field.

In the following, we consider the external field (only the z component is important here) to be of the form

$$E^{\mathrm{ext}}_z(\mathbf{r},t) = \mathcal{E}\sin(\theta_i)\cos(\omega_L t - k^L_x x - k^L_z z)\exp\left(-\frac{(t-t_0-k^L_x/\omega_L x - k^L_z/\omega_L z)^2}{2\tau^2}\right), \tag{A4}$$

where ω_L is the laser frequency and $\mathbf{k}_L=(k^L_x,0,k^L_z)$ is the corresponding wave vector. The Fourier transform of Eq. (A4) with respect to in-plane space coordinates and time can be expressed according to

$$\tilde{E}^{\mathrm{ext}}_z(\mathbf{q}_\parallel,z,\omega) = \hat{E}^{\mathrm{ext}}_z(\mathbf{q}_\parallel,z,\omega)\,\delta\left(q_x-\frac{\omega}{\omega_L}k^L_x\right)\delta(q_y) \tag{A5}$$

$$= \mathcal{E}^{\mathrm{ext}}_z(z,t)\,\delta\left(q_x-\frac{\omega}{\omega_L}k^L_x\right)\delta(q_y). \tag{A6}$$

Note, that $\hat{E}^{\mathrm{ext}}_z(\mathbf{q}_\parallel,z,\omega)$ is only an abbreviation for the explicit function as we here are mainly interested in the part with the delta function. Inserting Eq. (A5) in the (time) Fourier transform of Eq. (A3), we find that only intersubband coherences with $\mathbf{q}_\parallel=(\omega/\omega_L)\mathbf{k}^L_\parallel$ are driven directly by the external field. Assuming that these contributions are the dominant ones, we approximate the macroscopic polarization according to

$$\mathbf{P}(\mathbf{r},t) \approx \frac{1}{\sqrt{2\pi}}\int_{-\infty}^{\infty}d\omega\sum_{\mathbf{q}_\parallel}\hat{\mathbf{P}}(z,\omega)e^{i(\mathbf{q}_\parallel\cdot\mathbf{r}_\parallel-\omega t)}\delta_{\mathbf{q}_\parallel,(\omega/\omega_L)\mathbf{k}^L_\parallel}$$

with

$$\hat{\mathbf{P}}(z,\omega) = \frac{1}{A}\sum_{\mathbf{k}_\parallel,m}[p^{(m)}_{\mathbf{k}_\parallel-(\omega/\omega_L)\mathbf{k}^L_\parallel,\mathbf{k}_\parallel}(\omega)+\mathrm{c.c.}]\mathbf{d}_{12}(z). \tag{A7}$$

For the parameter range considered, we have $\mathbf{k}^L_\parallel \ll \mathbf{k}_\parallel$ and expect the dominant contributions to the intersubband coherence for $\omega\approx\omega_L$. Thus, we can simplify Eq. (A7) further

$$\hat{\mathbf{P}}(z,\omega) \approx \frac{1}{A}\sum_{\mathbf{k}_\parallel,m}\left[p^{(m)}_{\mathbf{k}_\parallel}(\omega)+\mathrm{c.c.}\right]\mathbf{d}_{12}(z)$$

and find that the macroscopic polarization is mainly composed of intersubband coherences which are diagonal in $\mathbf{k}_\parallel$.

APPENDIX B

The various contributions to Eq. (9) are given by

$$\left.\frac{d}{dt}p_{\mathbf{k}_\parallel}\right|_0 = -\frac{\mathrm{i}}{\hbar}(\epsilon_{2,\mathbf{k}_\parallel}-\epsilon_{1,\mathbf{k}_\parallel})p_{\mathbf{k}_\parallel}$$

$$\left.\frac{d}{dt}p_{\mathbf{k}_\parallel}\right|_{\mathrm{HF}} = \frac{\mathrm{i}}{\hbar}\sum_{\mathbf{q}_\parallel}\{[(V^{2222}_{q_\parallel}-V^{2112}_{q_\parallel})n^2_{\mathbf{k}_\parallel+\mathbf{q}_\parallel}-(V^{1111}_{q_\parallel} - V^{2112}_{q_\parallel})n^1_{\mathbf{k}_\parallel+\mathbf{q}_\parallel}]p_{\mathbf{k}_\parallel}+(V^{1212}_{q_\parallel}p_{\mathbf{k}_\parallel-\mathbf{q}_\parallel}+V^{2112}_{q_\parallel}p^*_{\mathbf{k}_\parallel-\mathbf{q}_\parallel}) \times(n^1_{\mathbf{k}_\parallel}-n^2_{\mathbf{k}_\parallel})-2V^{2112}_0(p_{\mathbf{q}_\parallel}+p^*_{\mathbf{q}_\parallel})(n^1_{\mathbf{k}_\parallel}-n^2_{\mathbf{k}_\parallel})\},$$

$$\left.\frac{d}{dt}n^i_{\mathbf{k}_\parallel}\right|_{\mathrm{HF}} = \frac{\mathrm{i}}{\hbar}\sum_{\mathbf{q}_\parallel}\{[(V^{ijij}_{q_\parallel}p^{ii}_{\mathbf{k}_\parallel-\mathbf{q}_\parallel}+V^{jiij}_{q_\parallel}p^{ij}_{\mathbf{k}_\parallel-\mathbf{q}_\parallel})p^{ij}_{\mathbf{k}_\parallel}-\mathrm{c.c.}] -[V^{jiij}_0(p^{ij}_{\mathbf{q}_\parallel}+p^{ji}_{\mathbf{q}_\parallel})p^{ij}_{\mathbf{k}_\parallel}-\mathrm{c.c.}]\}.$$

$$\left.\frac{d}{dt}p_{\mathbf{k}_\parallel}\right|_{\text{cp-scatt}} = -\frac{\pi}{\hbar}\Xi_d(p_{\mathbf{k}_\parallel})+\frac{\pi}{\hbar}\sum_{\mathbf{q}}\Xi_{nd}(p^{ij}_{\mathbf{k}_\parallel+\mathbf{q}_\parallel})+\frac{\pi}{\hbar}\Xi_{nl},$$

For convenience the index (m) denoting the quantum well number has been suppressed and $p^{ii}_{\mathbf{k}_\parallel}=\langle a^{\dagger}_{j,\mathbf{k}_\parallel}a_{i,\mathbf{k}_\parallel}\rangle$ has been introduced. Note that the summation over the spin indices has already been performed here and thus only the wave vector $\mathbf{k}$ includes a spin index. The Coulomb and Froehlich matrix elements and the scattering contributions $\Xi_d(p_{\mathbf{k}_\parallel}),\Xi_{nd}(p^{ij}_{\mathbf{k}_\parallel+\mathbf{q}_\parallel})$ and Ξ_{nl} are defined in Ref. 15.

[1] L. Allen and J. H. Eberly, *Optical Resonance and Two-Level Atoms* (Dover, New York, 1987).

[2] P. Borri, W. Langbein, S. Schneider, U. Woggon, R. L. Sellin, D. Ouyang, and D. Bimberg, Phys. Status Solidi B **233**, 391 (2002).

[3] J. Förstner, C. Weber, J. Danckwerts, and A. Knorr, Phys. Rev. Lett. **91**, 127401 (2003).

[4] F. T. Vasko, Phys. Rev. B **70**, 073305 (2004).

[5] G. Y. Slepyan, A. Magyarov, S. A. Maksimenko, A. Hoffmann, and D. Bimberg, Phys. Rev. B **70**, 045320 (2004).

[6] R. Binder, S. W. Koch, M. Lindberg, N. Peyghambarian, and W. Schäfer, Phys. Rev. Lett. **65**, 899 (1990).

[7] S. T. Cundiff, A. Knorr, J. Feldmann, S. W. Koch, E. O. Göbel, and H. Nickel, Phys. Rev. Lett. **73**, 1178 (1994).

[8] A. Schulzgen, R. Binder, M. E. Donovan, M. Lindberg, K. Wundke, H. M. Gibbs, G. Khitrova, and N. Peyghambarian, Phys. Rev. Lett. **82**, 2346 (1999).

[9] C. W. Luo, K. Reimann, M. Woerner, T. Elsaesser, R. Hey, and K. H. Ploog, Phys. Rev. Lett. **92**, 047402 (2004).

[10] A. A. Batista and D. S. Citrin, Phys. Rev. Lett. **92**, 127404

(2004).
[11] D. McPeake, F. T. Vasko, and E. P. O'Reilly, Phys. Rev. B **68**, 193306 (2003).
[12] T. Shih, K. Reimann, M. Woerner, T. Elsaesser, I. Waldmüller, A. Knorr, R. Hey, and K. H. Ploog, Phys. Rev. B **72**, 195338 (2005).
[13] D. E. Nikonov, A. Imamoğlu, L. V. Butov, and H. Schmidt, Phys. Rev. Lett. **79**, 4633 (1997).
[14] I. Waldmüller, M. Woerner, J. Förstner, and A. Knorr, Phys. Status Solidi B **238**, 474 (2003).
[15] I. Waldmüller, J. Förstner, S. C. Lee, A. Knorr, M. Woerner, K. Reimann, R. A. Kaindl, T. Elsaesser, R. Hey, and K. H. Ploog, Phys. Rev. B **69**, 205307 (2004).
[16] J. Li and C. Z. Ning, Phys. Rev. B **70**, 125309 (2004).
[17] U. Ekenberg, Phys. Rev. B **40**, 7714 (1989).
[18] T. Kuhn, in *Theory of Transport Properties of Semiconductor Nanostructures*, edited by E. Schöll (Chapman and Hall, London, 1998), p. 173.
[19] I. Waldmüller, J. Förstner, and A. Knorr, in *Nonequilibrium Physics at Short Time Scales*, edited by K. Morawetz (Springer, Berlin, 2004).
[20] J. E. Sipe, J. Opt. Soc. Am. B **4**, 481 (1987).
[21] B. Robertson, Phys. Rev. **144**, 151 (1966); E. Fick and G. Sauermann, *The Quantum Statistics of Dynamical Processes* (Springer, Berlin, 1990).
[22] S. Butscher, J. Forstner, I. Waldmüller, and A. Knorr, Phys. Status Solidi B **241**, R49 (2004).
[23] A. Liu, Phys. Rev. B **50**, 8569 (1994).